
Augmentation-Free Graph Contrastive Learning

Haonan Wang

University of Illinois Urbana-Champaign
haonan3@illinois.edu

Jieyu Zhang

University of Washington
jieyuz2@cs.washington.edu

Qi Zhu

University of Illinois Urbana-Champaign
qiz3@illinois.edu

Wei Huang *

University of Technology Sydney
wei.huang.uts@gmail.com

Abstract

Graph contrastive learning (GCL) is the most representative and prevalent self-supervised learning approach for graph-structured data. Despite its remarkable success, existing GCL methods highly rely on an augmentation scheme to learn the representations invariant across different augmentation views. In this work, we revisit such a convention in GCL through examining the effect of augmentation techniques on graph data via the lens of spectral theory. We found that graph augmentations preserve the low-frequency components and perturb the middle- and high-frequency components of the graph, which contributes to the success of GCL algorithms on homophilic graphs but hinder its application on heterophilic graphs, due to the high-frequency preference of heterophilic data. Motivated by this, we propose a novel, theoretically-principled, and augmentation-free GCL method, named AF-GCL, that (1) leverages the features aggregated by Graph Neural Network to construct the self-supervision signal instead of augmentations and therefore (2) is less sensitive to the graph homophily degree. Theoretically, We present the performance guarantee for AF-GCL as well as an analysis for understanding the efficacy of AF-GCL. Extensive experiments on 14 benchmark datasets with varying degrees of heterophily show that AF-GCL presents competitive or better performance on homophilic graphs and outperforms all existing state-of-the-art GCL methods on heterophilic graphs with significantly less computational overhead.

1 Introduction

Graph Neural Networks (GNNs) [1, 2, 3, 4] have attracted great attention due to their success in various applications involving graph-structured data, such as node classification [1], edge prediction [5], graph classification [2], etc. Most of these tasks are semi-supervised and therefore require a certain number of labels to guide the learning process. However, in many real-world applications (e.g., chemistry and healthcare), labels are scarcely available. Self-supervised learning (SSL), as an appropriate paradigm for such label-scarce settings, has been extensively studied in Computer Vision (CV). Besides, contrastive learning, the most representative SSL technique, has achieved state-of-the-art performance [6]. This has motivated the self-supervised learning, especially contrastive learning, approaches [7] on graph data.

Contrastive learning is essentially learning representations invariant to data augmentations which are thoroughly explored on visual data [8, 9]. Leveraging the same paradigm, Graph Contrastive Learning (GCL) encourages the representations to contain as less information about the way the inputs are transformed as possible during training, i.e. to be invariant to a set of manually specified transformations.

*Corresponding Author

However, the irregular structure of the graph complicates the adaptation of augmentation techniques used on images, and prevents the extending of theoretical analysis for visual contrastive learning to a graph setting. In recent years, many works [10, 11, 12, 13, 14, 15] focus on the empirical design of hand-craft graph augmentations for graph contrastive learning from various levels, including node dropping, edge perturbation, attribute masking, subgraph [10], and graph diffusion [12]. Although experiments have demonstrated the effectiveness of the GCL algorithms [16], those empirical studies are limited to the homophilic graphs, where the linked nodes are likely from the same class, e.g. social network and citation networks [17]. In heterophilic graphs, similar nodes are often far apart (e.g., the majority of people tend to connect with people of the opposite gender [18] in dating networks), which urges the investigation on the generalization of GCL frameworks on both homophilic and heterophilic graphs.

To fill this gap, we first investigate the empirical success of GCL algorithms. As discussed in [10, 16], existing GCL algorithms learn invariant representations across different graph augmentation views. In this work, we take a closer look at what information is preserved or perturbed by commonly used graph augmentations. By analyzing the graph structure and features from the view of frequency, we observe that graph augmentations mainly preserve low-frequency information and corrupt middle and high-frequency information of the graph. By enforcing the model to learn representations invariant to the perturbations through maximizing the agreement between a graph and its augmentations, the learned representations will only retain the low-frequency information. As demonstrated in [19], the low-frequency information is critical for the homophilic graph. However, for heterophilic graph, the low-frequency information is insufficient for learning effective representations. Under this circumstance, the middle and high-frequency information, capturing the difference between nodes, may be more effective [20, 21], but typically overlooked by existing GCL algorithms. Thus, it rises a natural question, that is, *is it possible to design a generic graph contrastive learning method effective on both homophilic and heterophilic graphs?*

In this work, we answer the above question affirmatively by providing a new perspective of achieving SSL on graphs. Specifically, based on our analysis of the concentration property of aggregated features on both homophilic and heterophilic graphs, we propose a novel *augmentation-free graph contrastive learning* method, named AF-GCL. Different from the large body of previous works on the graph contrastive learning, in which the construction of self-supervision signals is heavily relying on graph augmentation, AF-GCL constructs positive/negative pairs based on the aggregated node features and directly optimizes the distance of representations in high-dimensional space. As a simple yet effective approach, AF-GCL frees the model from dual branch design and graph augmentations, which enable the proposed method to easily scale to large graphs.

In addition, we present a theoretical guarantee for the performance of embedding learned by AF-GCL in downstream tasks, and our theoretical analysis provides an understanding of when and why AF-GCL can work well. Experimental results show that AF-GCL outperforms state-of-the-art GCL algorithms on 4 out of 8 homophilic graph benchmarks and achieve competitive performance on the remaining 4 datasets. Besides, as the first method which can work well on both homophilic and heterophilic graphs, AF-GCL outperforms all those GCL algorithms and supervised methods on 5 out of 6 heterophilic graph benchmarks and achieves competitive performance on the remaining one. Furthermore, we analyze the computational complexity of AF-GCL and empirically show that our method performs well with significantly less computational overhead. Our contribution could be summarized as:

- We first analyze the efficacy of graph augmentation techniques for GCL as well as its limitations from a spectral point of view. We show that augmentation-based GCL is sensitive to the graph’s homophily degree.
- We then illustrate the concentration property of representations obtained by the neighborhood feature aggregation, which in turn inspires our novel augmentation-free graph contrastive learning method, AF-GCL.
- We further present a theoretical guarantee for the performance of AF-GCL, as well as the analyses of AF-GCL’s robustness to the graph’s homophily degree.
- Experimental results show that without complex designs, compared with SOTA GCL methods, AF-GCL achieves competitive or better performance on 8 homophilic graph benchmarks and 6 heterophilic graph benchmarks, with significantly less computational overhead.

2 Related Work

2.1 Graph Contrastive Learning

Contrastive learning aims to learn consistent representations under proper transformations and has been widely applied to the visual domain. Graph Contrastive Learning (GCL) leverages the idea of CL on the graph data. However, due to the complex, irregular structure of graph data, it is more challenging to design appropriate strategies for constructing positive and negative samples on the graph than that on visual or textual data. Regarding graph augmentation, many previous studies [10, 11, 12, 16, 13, 14, 15] propose data augmentation techniques for general graph-structured data, e.g., attribute masking, edge removing, edge adding, subgraph, graph diffusion. Specifically, MVGRL [12] employs graph diffusion to generate graph views with more global information; GCC [22] use the subgraph induced by random walks to serve as different views. GraphCL [10] study multiple augmentation methods for graph-level representation learning. GRACE [14] constructs node-node pairs by using edge removing and feature masking. GCA [13] proposes adaptive augmentation techniques to further consider important topology and attribute information. BGRL [23] gets rid of the design of negative pairs, but its design of positive pairs also relies on edge removing and feature masking. We summarized the graph augmentation methods employed by the representative GCL methods in Table 1. To the best of our knowledge, the current state-of-the-art GCL algorithms are highly reliant on graph augmentations, but none of the existing work studies the effect and limitation of current graph augmentation techniques in GCL.

Table 1: Summary of graph augmentations used by representative GCL models. Multiple* denotes multiple augmentation methods including edge removing, edge adding, node dropping and subgraph induced by random walks.

Method	Topology Aug.	Feature Aug.
MVGRL [12]	Diffusion	-
GCC [22]	Subgraph	-
GraphCL [10]	Multiple*	Feature Dropout
GRACE [14]	Edge Removing	Feature Masking
GCA [13]	Edge Removing	Feature Masking
BGRL [23]	Edge Removing	Feature Masking

2.2 Understanding Contrastive Learning

Previous theoretical guarantees for contrastive learning follow conditional independence assumption (or its variants) [24, 25, 26, 27]. Specifically, they assume the two contrastive views are independent conditioned on the label and show that contrastive learning can provably learn representations beneficial for downstream tasks. In addition, Wang et al.[28] investigated the representation geometry of supervised contrastive loss and showed that the contrastive loss favors data representation uniformly distributed over the unit sphere yet aligning across semantically similar samples. Haochen et al.[29] analyzed the contrastive learning on the augmented image dataset through the novel concept augmentation graph with a new loss function that performs spectral decomposition on the graph. However, all those theoretical analyses mainly focus on the classification problem with image datasets. Since graphs are far more complex due to the non-Euclidean property, the analysis for image classification cannot be trivially extended to graph setting.

Besides, on the other line of research, contrastive learning methods [30, 31, 11, 13] leveraging the information maximization principle (InfoMax) [32] aim to maximize the Mutual Information (MI) between the representation of one data point and that of its augmented version by contrasting positive pairs with negative-sampled counterparts. The key idea is that maximizing mutual information between representations extracted from multiple views can force the representations to capture information about higher-level factors (e.g., presence of certain objects or occurrence of certain events) that broadly affect the shared context. The employed loss functions, e.g. Information Noise Contrastive Estimation (InfoNCE) and Jensen-Shannon Divergence (JSD), are proved to be lower bounds of MI [33, 34, 35]. Although the idea of information maximization principle has been used in GCL domain [36, 15, 13], the higher-level factors invariant across different graph augmentation views is under-defined. In this work, we take a closer look at the graph augmentations via the lens of spectral theory and analyze what information is preserved in different augmentation views.

3 Preliminary

3.1 Notation

Let $\mathcal{G} = (\mathcal{V}, \mathcal{E})$ denote an undirected graph, where $\mathcal{V} = \{v_i\}_{i \in [N]}$ and $\mathcal{E} \subseteq \mathcal{V} \times \mathcal{V}$ denote the node set and the edge set respectively. We denote the number of nodes and edges as N and E , and the label of nodes as $\mathbf{y} \in \mathbb{R}^N$, in which $y_i \in [1, c]$, $c \geq 2$ is the number of classes. The associated node feature matrix denotes as $\mathbf{X} \in \mathbb{R}^{N \times F}$, where $\mathbf{x}_i \in \mathbb{R}^F$ is the feature of node $v_i \in \mathcal{V}$ and F is the input feature dimension. The adjacent matrix denotes as $\mathbf{A} \in \{0, 1\}^{N \times N}$, where $\mathbf{A}_{ij} = 1$ if $(v_i, v_j) \in \mathcal{E}$. Our objective is to unsupervisedly learn a GNN encoder $f_\theta : \mathbf{X}, \mathbf{A} \rightarrow \mathbb{R}^{N \times K}$ receiving the node features and graph structure as input, that produces node representations in low dimensionality, i.e., $K \ll F$. The representations can benefit the downstream supervised or semi-supervised tasks, e.g., node classification.

3.2 Homophilic and Heterophilic Graph

Various metrics have been proposed to measure the homophily degree of a graph. Here we adopt two representative metrics, namely, node homophily and edge homophily. The edge homophily [18] is the proportion of edges that connect two nodes of the same class:

$$h_{edge} = \frac{|\{(v_i, v_j) : (v_i, v_j) \in \mathcal{E} \wedge y_i = y_j\}|}{E}, \quad (1)$$

And the node homophily [37] is defined as,

$$h_{node} = \frac{1}{N} \sum_{v_i \in \mathcal{V}} \frac{|\{v_j : (v_i, v_j) \in \mathcal{E} \wedge y_i = y_j\}|}{|\{v_j : (v_i, v_j) \in \mathcal{E}\}|}, \quad (2)$$

which evaluates the average proportion of edge-label consistency of all nodes. They are all in the range of $[0, 1]$ and a value close to 1 corresponds to strong homophily while a value close to 0 indicates strong heterophily. As conventional, we refer the graph with high homophily degree as homophilic graph, and the graph with low homophily degree as heterophilic graph. And we provided the homophily degree of graph considered in this work in Table 7.

3.3 Graph Laplacian and Variants

We define the Laplacian matrix of the graph as $\mathbf{L} = \mathbf{D} - \mathbf{A}$, where $\mathbf{D} = \text{diag}(d_1, \dots, d_N)$, $d_i = \sum_j \mathbf{A}_{i,j}$. The symmetric normalized Laplacian, is defined as $\mathbf{L}_{sym} = \mathbf{D}^{-\frac{1}{2}} \mathbf{L} \mathbf{D}^{-\frac{1}{2}} = \mathbf{U} \mathbf{\Lambda} \mathbf{U}^\top$. Here $\mathbf{U} \in \mathbb{R}^{N \times N} = [\mathbf{u}_1, \dots, \mathbf{u}_N]$, where $\mathbf{u}_i \in \mathbb{R}^N$ denotes the i -th eigenvector of \mathbf{L}_{sym} and $\mathbf{\Lambda} = \text{diag}(\lambda_1, \dots, \lambda_N)$ is the corresponding eigenvalue matrix. λ_1 and λ_N be the smallest and largest eigenvalue respectively. The affinity (transition) matrices can be derived from the Laplacian matrix, $\mathbf{A}_{sym} = \mathbf{I} - \mathbf{L}_{sym} = \mathbf{D}^{-1/2} \mathbf{A} \mathbf{D}^{-1/2} = \mathbf{U}(\mathbf{I} - \mathbf{\Lambda})\mathbf{U}^\top$. The \mathbf{L}_{sym} has eigenvalue from 0 to 2 and is widely used in the design of spectral graph neural networks, such as Graph Convolutional Network (GCN) [1].

For the Laplacian matrix, the smaller eigenvalue is corresponding to the lower frequency [19]. Following the previous work [38], we define the decomposed components of \mathbf{L}_{sym} under different frequency bands as \mathbf{L}_{sym}^m which has eigenvalues in $[\lambda_N \cdot \frac{(m-1)}{M}, \lambda_N \cdot \frac{m}{M})$, and $m \in [1, M]$, $M \in \mathbb{Z}^+$ denotes the number of partition of the spectrum. More specifically, $\mathbf{L}_{sym}^m = \mathbf{U} \mathbf{\Lambda}^m \mathbf{U}^\top$, $\mathbf{\Lambda}^m = \text{diag}(\lambda_1^m, \dots, \lambda_N^m)$, where for $i \in [1, N]$,

$$\lambda_i^m = \begin{cases} \lambda_i, & \text{if } \lambda_i \in [\lambda_N \cdot \frac{(m-1)}{M}, \lambda_N \cdot \frac{m}{M}) \\ 0, & \text{otherwise} \end{cases},$$

Note, the sum of all decomposed components is equal to the symmetric normalized Laplacian matrix, $\mathbf{L}_{sym} = \sum_{m=0}^{\lceil N/M \rceil} \mathbf{L}_{sym}^m$.

4 Revisiting Graph Augmentations

Graph Contrastive Learning (GCL) aims to learn representations that are invariant to different augmentations. However, it is rarely studied what information is preserved or perturbed across

augmented graph views. In this section, we attempt to identify such information by examining the effect of graph augmentation techniques on graph geometric structure and node attributes from the spectral perspective.

4.1 Representative Augmentation Techniques

According to Table 1, the most commonly used four graph augmentation techniques for GCL are: attribute masking, edge adding, edge dropping [10] and graph diffusion [10].

- Attribute Masking: randomly masks a fraction of features for all the nodes.
- Edge Adding/Dropping: randomly adds/drops a fraction of edges from the original graph.
- Graph Diffusion: the Personalized PageRank (PPR) based graph diffusion is defined as, $\alpha (\mathbf{I} - (1 - \alpha)\mathbf{A}_{sym})^{-1}$, where α is the diffusion factor.

4.2 Effect of Augmentations on Geometric Structure

First, we investigate the effect of different augmentations, e.g., edge adding, edge dropping and graph diffusion, on adjacency matrix. As we introduced in Section 3.3, the graph Laplacians are widely used in GNNs, therefore we measure the difference of Laplacians caused by graph augmentations in different frequency bands. The m -th component symmetric normalized Laplacian is defined as \mathbf{L}_{sym}^m . Correspondingly, we denote the decomposed m -th symmetric normalized Laplacian for the augmented graph as $\tilde{\mathbf{L}}_{sym}^m$. To measure the impact of graph augmentations for different frequency components, we employ the Frobenius norm as the metric to measure the distance, $\|\mathbf{L}_{sym}^m - \tilde{\mathbf{L}}_{sym}^m\|_F$. The results of edge dropping on two homophilic graphs, e.g., Cora and CiteSeer [39, 40], and two heterophilic graphs, e.g., Chameleon and Squirrel [41], are summarized in Figure 1 and the results of other graph augmentation techniques are in Appendix 9.3. We observed that graph augmentations have less impact on low-frequency components and more impact on middle and high-frequency components. Our conclusion is aligned with the previous works [38, 42] in the graph adversarial attack domain, in which they find that, for the graph structure modification, perturbations on the low-frequency components are smaller than that in the middle or high-frequency ones.

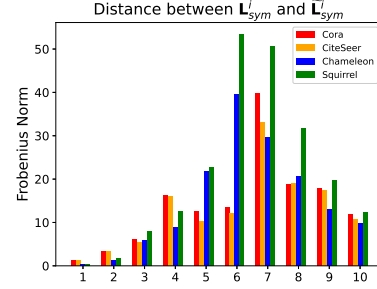


Figure 1: Frobenius distance between the decomposed symmetric normalized Laplacian matrices of the original graph and the augmented graph with 20% edge dropping. The experiment is independent conducted 10 times and the average value is reported.

4.3 Effect of Augmentations on Features

To further study the effect of the commonly used graph augmentation method, attribute masking, on node attribute from spectral view. We denote the Fourier transform and inverse Fourier transform as $\mathcal{F}(\cdot)$ and $\mathcal{F}^{-1}(\cdot)$. We use $\mathbf{H}^{\mathcal{F}}$ to denote the transformed node features. Therefore, we have $\mathbf{H}^{\mathcal{F}} = \mathcal{F}(\mathbf{X})$ and $\mathbf{X} = \mathcal{F}^{-1}(\mathbf{H}^{\mathcal{F}})$. We decompose the node attribute $\mathbf{X} = \{\mathbf{X}^l, \mathbf{X}^h\}$, where \mathbf{X}^l and \mathbf{X}^h denote the low-frequency and high-frequency components of \mathbf{X} respectively. We have the following four equations:

$$\begin{aligned} \mathbf{H}^{\mathcal{F}} &= \mathcal{F}(\mathbf{X}), & \mathbf{H}^l, \mathbf{H}^h &= t(\mathbf{H}^{\mathcal{F}}; R), \\ \mathbf{X}^l &= \mathcal{F}^{-1}(\mathbf{H}^l), & \mathbf{X}^h &= \mathcal{F}^{-1}(\mathbf{H}^h), \end{aligned}$$

where $t(\cdot; R)$ denotes a thresholding function that separates the low and high frequency components from $\mathbf{H}^{\mathcal{F}}$ according to a hyperparameter, m . Because the column of $\mathbf{H}^{\mathcal{F}}$ in the left is corresponding to the low frequency component, we define $t(\cdot; m)$ as:

$$\mathbf{H}_{ij}^l = \begin{cases} \mathbf{H}_{ij}^{\mathcal{F}}, & \text{if } j \leq R \\ 0, & \text{otherwise} \end{cases}, \quad \mathbf{H}_{ij}^h = \begin{cases} 0, & \text{if } j \leq R \\ \mathbf{H}_{ij}^{\mathcal{F}}, & \text{otherwise} \end{cases}. \quad (3)$$

Table 2: Distance between original node features and augmented node features with 30% attribute dropping. We set $R = 0.8 \times F$.

	F-Low	F-High
Cora	0	7.949
CiteSeer	0	5.609
Chameleon	0	12.566
Squirrel	0	15.836

Further, we denote the node attribute with attribute masking as $\tilde{\mathbf{X}}$ and its corresponding low and high frequency components as $\tilde{\mathbf{X}}^l, \tilde{\mathbf{X}}^h$. We investigate the influence of attribute masking on node features by computing the Frobenius distance of matrix, and denote $\|\mathbf{X}^l - \tilde{\mathbf{X}}^l\|_F$ as F-norm-low and $\|\mathbf{X}^h - \tilde{\mathbf{X}}^h\|_F$ as F-norm-high. The results on four datasets are summarized in Table 2. We surprisingly find that the attribute masking will always affect the high frequency component.

4.4 Concluding Remarks

As demonstrated by previous works [20, 21], for heterophilic graphs, the information carried by high-frequency components is more effective for downstream classification performance. However, as we analyzed, the middle- and high-frequency information are perturbed by commonly used graph augmentation techniques. With the information maximization objective, only the invariant information (low-frequency) is encouraged to be captured by the learned embedding [10]. Although existing graph augmentation algorithms promote the success of GCL on traditional (homophilic) benchmarks, they result in sub-optimal representations when the high-frequency information is crucial (heterophilic graphs).

5 Methodology

As analyzed in the previous section, the aforementioned graph augmentation techniques are less effective for heterophilic graphs (see also experimental results in Table 4). To design a universal self-supervision signal, we are motivated to analyze the concentration property of aggregated node feature \mathbf{Z} (Section 5.1) for both homophilic and heterophilic graphs. Namely, nodes of the same class are closer with each other under different degree of homophily. Leveraging the concentration property, we propose an augmentation-free method (Section 5.2), AF-GCL, to construct positive and negative pairs for contrastive learning.

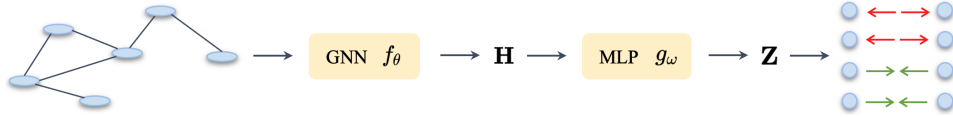


Figure 2: Overview of the proposed AF-GCL.

5.1 Analysis of Aggregated Features

We follow prior work [43, 44] to assume that the node feature follows the Gaussian mixture model [45]. For simplicity, we focus on the two-classes problem. Conditional on the (binary-) label y and a latent vector $\mathbf{u} \sim \mathcal{N}(\mathbf{0}, \mathbf{I}_F/F)$, the features are governed by:

$$\mathbf{x}_i = y_i \mathbf{u} + \frac{\vec{\mu}_i}{\sqrt{F}}, \quad (4)$$

where random variable $\vec{\mu}_i \in \mathbb{R}^F$ has independent standard normal entries and $y_i \in \{-1, 1\}$ representing latent classes. In other words, the features of nodes with class y_i follow the same distribution depending on y_i , i.e., $\mathbf{x}_i \sim P_{y_i}(\mathbf{x})$. Furthermore, we make an assumption on the neighborhood patterns,

Assumption 1 For node i , its neighbor's labels are independently sampled from a distribution $P(y_i)$.

The above assumption implies that the neighbor's label is generated from a distribution only dependent on the label of the central node, which contains both cases of homophily and heterophily. With this assumption, we prove the following Lemma 1 that all aggregated node features with the same label have the same embedding regardless of homophily or heterophily. Specifically, we define learned embedding through a GCN and MLP by \mathbf{Z} as shown in Figure 2, and \mathbf{Z}_i is the learned embedding with respect to input \mathbf{x}_i . To simplify the analysis, we introduce \mathbf{W} being the equivalent linear weight after dropping non-linearity in GCN and MLP.

Lemma 1 (Adaption of Theorem 1 in [46]) Consider a graph G following the assumption 1 and Eq. (4), then the expectation of embedding is given by

$$\mathbb{E}[\mathbf{Z}_i] = \mathbf{W} \mathbb{E}_{y \sim P(y_i), \mathbf{x} \sim P_y(\mathbf{x})}[\mathbf{x}], \quad (5)$$

Furthermore, with probability at least $1 - \delta$ over the distribution for graph, we have:

$$\|\mathbf{Z}_i - \mathbb{E}[\mathbf{Z}_i]\|_2 \leq \sqrt{\frac{\sigma_{\max}^2(\mathbf{W}) F \log(2F/\delta)}{2\mathbf{D}_{ii}\|\mathbf{x}\|_{\psi_2}}}, \quad (6)$$

where the sub-gaussian norms $\|\mathbf{x}\|_{\psi_2} \equiv \min_i \|\mathbf{x}_{i,d}\|_{\psi_2}$, $d \in [1, F]$ and $\sigma_{\max}^2(\mathbf{W})$ is the largest singular value of \mathbf{W} , because each dimension in feature is independently distributed.

We leave the proof of the above lemma in Appendix 9.4.1. The above lemma indicates that, for any graph where the feature and neighborhood pattern of each node is sampled from the distributions depending on the node label, the GCN model is able to map nodes with the same label to an area centered around the expectation in the embedding space.

5.2 Augmentation-Free Graph Contrastive Learning (AF-GCL)

The above theoretical analysis reveals that, for each class, the embedding obtained from neighbor aggregation will concentrate toward the expectation of embedding belonging to the class. Inspired by this, we design the self-supervision signal based on the obtained embedding and propose a novel augmentation-free graph contrastive learning algorithm, AF-GCL, which selects similar nodes as positive node pairs. As shown in the previous analysis, the concentration property is independent with homophily and heterophily assumptions, therefore AF-GCL generalizes well on both homophilic and heterophilic graphs. And the augmentation-free design makes AF-GCL get rid of the commonly adapted dual-branch design [16] and significantly reduce the computational overhead.

As shown in Figure 2, in each iteration, the proposed framework first encodes the graph with a graph encoder f_θ denoted by $\mathbf{H} = f_\theta(\mathbf{X}, \mathbf{A})$. Notably, our framework allows various choices of the network architecture without any constraints. Then, a MLP projection head with L2-normalization, g_ω , is employed to project the node embedding into the hidden representation $\mathbf{Z} = g_\omega(\mathbf{H})$. At each iteration, b nodes are sampled to form the seed node set S ; and their surrounding T -hop neighbors consist the node pool, P . For each seed node $v_i \in S$, the top- K_{pos} nodes with highest similarity from the node pool are selected as positive set for it, and denote as $S_{pos}^i = \{v_i, v_i^1, v_i^2, \dots, v_i^{K_{pos}}\}$. Specifically,

$$v_i^1, v_i^2, \dots, v_i^{K_{pos}} = \arg \max_{v_j \in P} (\mathbf{Z}_i^\top \mathbf{Z}_j, K_{pos}), \quad (7)$$

where $\arg \max(\cdot, K_{pos})$ denotes the operator for the top- K_{pos} selection, and because the hidden representation is normalized, the inner product of hidden representations is equal to the cosine similarity. The framework is optimized with the following objective:

$$\mathcal{L}_{gcl} = -2 \mathbb{E}_{\substack{v_i \sim Uni(\mathcal{V}) \\ v_i^+ \sim Uni(S_{pos}^i)}} [\mathbf{Z}_i^\top \mathbf{Z}_{i^+}] + \mathbb{E}_{\substack{v_j \sim Uni(\mathcal{V}) \\ v_k \sim Uni(\mathcal{V})}} [(\mathbf{Z}_j^\top \mathbf{Z}_k)^2]. \quad (8)$$

Algorithm 1: Augmentation-Free Graph Contrastive Learning (AF-GCL).

Input: Graph neural network f_θ , MLP g_ω , input adjacency matrix \mathbf{A} , node features \mathbf{X} , batch size b , number of hops T , number of positive nodes K_{pos} .

for epoch $\leftarrow 1, 2, \dots$ **do**

1. Obtain the node embedding, $\mathbf{H} = f_\theta(\mathbf{X}, \mathbf{A})$.

2. Obtain the hidden representation, $\mathbf{Z} = g_\omega(\mathbf{H})$.

3. Sample b nodes for seed node set S .

4. Construct the node pool P with the T -hop neighbors of each node in the node set S .

5. Select top- K_{pos} similar nodes for every $v_i \in S$ to form the positive node set S_{pos}^i .

6. Compute the contrastive objective with Eq. (8) and update parameters by applying stochastic gradient.

end for

return Final model f_θ .

where the node v_{i+} , v_j and v_k are uniformly sampled from their corresponding set. Overall, the training algorithm AF-GCL is summarized in Algorithm 1.

6 Theoretical Analyses

In this section, we aim to derive a performance guarantee for AF-GCL. Note that we leave all the proof in the appendix. First, we introduce the concept of *transformed graph* as follows, which is constructed based on the original graph and the selected positive pairs.

Definition 1 (Transformed Graph) *Given the original graph \mathcal{G} and its node set \mathcal{V} , the transformed graph, $\hat{\mathcal{G}}$, has the same node set \mathcal{V} but with the selected positive pairs by AF-GCL as the edge set, $\hat{\mathcal{E}} = \bigcup_i \{(v_i, v_i^k) \mid k=1 \dots K_{pos}\}$.*

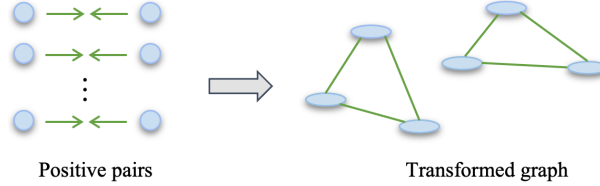


Figure 3: Transformed Graph formed with Positive Pairs.

We also illustrate the transformed graph with Figure 3. And we denote the adjacency matrix of transformed graph as $\hat{\mathbf{A}} \in \{0, 1\}^{N \times N}$, the number of edges as \hat{E} , and the symmetric normalized matrix as $\hat{\mathbf{A}}_{sym} = \hat{\mathbf{D}}^{-1/2} \hat{\mathbf{A}} \hat{\mathbf{D}}^{-1/2}$. Then we show that optimizing a model with the contrastive loss (Equation (8)) is equivalent to the matrix factorization over the transformed graph, as stated in the following lemma:

Lemma 2 *Denote the learnable embedding for matrix factorization as $\mathbf{F} \in \mathbb{R}^{N \times K}$. Let $\mathbf{F}_i = f_\theta \circ g_\omega(v_i)$. Then, the matrix factorization loss function \mathcal{L}_{mf} is equivalent to the contrastive loss (Equation (8)), up to an additive constant:*

$$\mathcal{L}_{mf}(\mathbf{F}) = \left\| \hat{\mathbf{A}}_{sym} - \mathbf{F} \mathbf{F}^\top \right\|_F^2 = \mathcal{L}_{gcl} + const \quad (9)$$

The above lemma bridges the graph contrastive learning and the graph matrix factorization and therefore allows us to provide the performance guarantee of AF-GCL by leveraging the power of matrix factorization. In addition, we provide an analysis for the inner product of hidden representations, namely $\mathbf{Z}_i^\top \mathbf{Z}_j$:

Theorem 1 *Consider a graph G following the assumption 1 and Eq. (4). Then with probability at least $1 - \delta$ we have,*

$$|\mathbf{Z}_i^\top \mathbf{Z}_j - \mathbb{E}[\mathbf{Z}_i^\top \mathbf{Z}_j]| \leq \sqrt{\frac{\sigma_{\max}^2(\mathbf{W}^\top \mathbf{W}) \log(2N^2/\delta)}{2D^2 \|\mathbf{x}^2\|_{\psi_1}}} \quad (10)$$

where $D = \min_i D_{ii}$ and sub-exponential norms $\|\mathbf{x}^2\|_{\psi_1} = \min_i \|\mathbf{x}_{i,d}^2\|_{\psi_1}$ for $d \in [1, F]$.

By above theorem, we demonstrate that inner product of hidden representations approximates to its expectation with a high probability. Furthermore, suppose that the expected homophily over distribution of graph feature and label, i.e., $y \sim P(y_i)$, $\mathbf{x} \sim P_y(\mathbf{x})$, through similarity selection satisfies $\mathbb{E}[h_{edge}(\hat{\mathcal{G}})] = 1 - \bar{\phi}$. Here $\bar{\phi} = \mathbb{E}_{y \sim P(y_i), \mathbf{x} \sim P_y(\mathbf{x})} [y_i \neq y_j]$. Then combining with Lemma 2 and Theorem 1, we can now provide a theoretical guarantee for AF-GCL:

Theorem 2 *Let $f_{gcl}^* \in \arg \min_{f: \mathcal{X} \rightarrow \mathbb{R}^K}$ be a minimizer of the GCL loss, \mathcal{L}_{gcl} . Then there exists a linear classifier $\mathbf{B}^* \in \mathbb{R}^{c \times K}$ with norm $\|\mathbf{B}^*\|_F \leq 1/(1 - \lambda_K)$ such that, with a probability at least $1 - \delta$*

$$\mathbb{E}_{v_i} \left[\|\vec{y}_i - \mathbf{B}^* f_{gcl}^*(v_i)\|_2^2 \right] \leq \frac{\bar{\phi}}{\lambda_{K+1}} + \sqrt{\frac{\sigma_{\max}^2(\mathbf{W}^\top \mathbf{W}) \log(2N^2/\delta)}{2D^2 \|\mathbf{x}^2\|_{\psi_1} \hat{\lambda}_{K+1}^2}}, \quad (11)$$

Table 3: Graph Contrastive Learning on Homophilic Graphs. The highest performance of unsupervised models is highlighted in boldface. OOM indicates Out-Of-Memory on a 32GB GPU.

Models	Cora	CiteSeer	PubMed	WikiCS	Amz-Comp.	Amz-Photo	Coauthor-CS	Coauthor-Phy.
MLP	47.92 \pm 0.41	49.31 \pm 0.26	69.14 \pm 0.34	71.98 \pm 0.42	73.81 \pm 0.21	78.53 \pm 0.32	90.37 \pm 0.19	93.58 \pm 0.41
GCN	81.54 \pm 0.68	70.73 \pm 0.65	79.16 \pm 0.25	93.02 \pm 0.11	86.51 \pm 0.54	92.42 \pm 0.22	93.03 \pm 0.31	95.65 \pm 0.16
DeepWalk	70.72 \pm 0.63	51.39 \pm 0.41	73.27 \pm 0.86	74.42 \pm 0.13	85.68 \pm 0.07	89.40 \pm 0.11	84.61 \pm 0.22	91.77 \pm 0.15
Node2vec	71.08 \pm 0.91	47.34 \pm 0.84	66.23 \pm 0.95	71.76 \pm 0.14	84.41 \pm 0.14	89.68 \pm 0.19	85.16 \pm 0.04	91.23 \pm 0.07
GAE	71.49 \pm 0.41	65.83 \pm 0.40	72.23 \pm 0.71	73.97 \pm 0.16	85.27 \pm 0.19	91.62 \pm 0.13	90.01 \pm 0.71	94.92 \pm 0.08
VGAE	77.31 \pm 1.02	67.41 \pm 0.24	75.85 \pm 0.62	75.56 \pm 0.28	86.40 \pm 0.22	92.16 \pm 0.12	92.13 \pm 0.16	94.46 \pm 0.13
DGI	82.34 \pm 0.71	71.83 \pm 0.54	76.78 \pm 0.31	75.37 \pm 0.13	84.01 \pm 0.52	91.62 \pm 0.42	92.16 \pm 0.62	94.52 \pm 0.47
GMI	82.39 \pm 0.65	71.72 \pm 0.15	79.34 \pm 1.04	74.87 \pm 0.13	82.18 \pm 0.27	90.68 \pm 0.18	OOM	OOM
MVGRL	83.45 \pm 0.68	73.28 \pm 0.48	80.09 \pm 0.62	77.51 \pm 0.06	87.53 \pm 0.12	91.74 \pm 0.08	92.11 \pm 0.14	95.33 \pm 0.05
GRACE	81.92 \pm 0.89	71.21 \pm 0.64	80.54 \pm 0.36	78.19 \pm 0.10	86.35 \pm 0.44	92.15 \pm 0.25	92.91 \pm 0.20	95.26 \pm 0.22
GCA	82.07 \pm 0.10	71.33 \pm 0.37	80.21 \pm 0.39	<u>78.40 \pm 0.13</u>	87.85 \pm 0.31	92.49 \pm 0.11	92.87 \pm 0.14	<u>95.68 \pm 0.05</u>
BGRL	81.44 \pm 0.72	71.82 \pm 0.48	80.18 \pm 0.63	76.96 \pm 0.61	89.62 \pm 0.37	93.07 \pm 0.34	92.67 \pm 0.21	95.47 \pm 0.28
AF-GCL	<u>83.32 \pm 0.13</u>	<u>72.09 \pm 0.42</u>	<u>80.25 \pm 0.75</u>	78.95 \pm 0.51	<u>89.27 \pm 0.25</u>	<u>92.89 \pm 0.49</u>	92.91 \pm 0.10	95.75 \pm 0.15

Table 4: Graph Contrastive Learning on Heterophilic Graphs. The highest performance of unsupervised models is highlighted in boldface. OOM indicates Out-Of-Memory on a 32GB GPU.

Models	Chameleon	Squirrel	Actor	Twitch-DE	Twitch-gamers	Genius
MLP	47.59 \pm 0.73	31.67 \pm 0.61	25.62 \pm 0.59	69.44 \pm 0.17	60.71 \pm 0.18	86.62 \pm 0.11
GCN	66.45 \pm 0.48	53.03 \pm 0.57	30.28 \pm 0.60	73.43 \pm 0.07	62.74 \pm 0.03	87.72 \pm 0.18
DeepWalk	60.18 \pm 1.25	45.83 \pm 0.95	27.81 \pm 0.81	72.40 \pm 0.39	62.63 \pm 0.16	74.65 \pm 0.13
Node2vec	31.23 \pm 0.98	29.99 \pm 0.81	28.46 \pm 0.45	71.38 \pm 0.15	62.29 \pm 0.11	72.51 \pm 0.14
GAE	52.85 \pm 0.41	41.83 \pm 0.79	31.02 \pm 1.42	68.81 \pm 0.35	57.18 \pm 0.25	80.56 \pm 0.15
VGAE	57.28 \pm 0.12	46.31 \pm 0.26	40.96 \pm 1.13	64.97 \pm 0.04	61.35 \pm 0.05	81.82 \pm 1.04
DGI	65.79 \pm 1.27	47.99 \pm 0.64	51.80 \pm 0.98	72.45 \pm 0.19	63.36 \pm 0.07	86.82 \pm 0.45
GMI	64.93 \pm 1.58	42.48 \pm 1.06	37.51 \pm 0.83	73.36 \pm 0.14	OOM	OOM
MVGRL	53.73 \pm 1.26	39.05 \pm 0.81	55.52 \pm 0.74	66.09 \pm 0.26	OOM	OOM
GRACE	66.14 \pm 0.53	53.09 \pm 0.86	50.06 \pm 0.62	73.79 \pm 0.22	OOM	OOM
GCA	66.21 \pm 0.77	53.34 \pm 0.79	49.83 \pm 0.41	<u>73.09 \pm 0.09</u>	OOM	OOM
BGRL	<u>67.29 \pm 0.70</u>	<u>55.48 \pm 0.63</u>	51.88 \pm 0.39	73.54 \pm 0.16	62.63 \pm 0.26	87.27 \pm 0.03
AF-GCL	69.34 \pm 0.81	57.46 \pm 0.48	58.83 \pm 0.82	74.15 \pm 0.09	<u>63.17 \pm 0.11</u>	91.61 \pm 0.29

$\hat{\lambda}_i$ are the i smallest eigenvalues of the symmetrically normalized Laplacian matrix of the transformed graph.

Interpreting the bound. The above theorem implies that if the transformed graph has a larger homophily degree (smaller $\bar{\phi}$), the bound of the prediction error will be lower. In other words, if the percentage of two nodes in positive pairs belonging to the same class is higher, the pre-trained GNN model tends to have better performance. Besides, the theorem reveals a trend that with the increase of hidden representation dimension K , a lower bound will be obtained.

7 Experiments

By extensive experiments, we show the efficacy, efficiency, and scalability of AF-GCL for both homophilic and heterophilic graphs. The results on homophilic and heterophilic graph benchmarks are presented in Section 7.1 and Section 7.2 respectively. The scalability and complexity analysis are given in Section 7.3. In Section 7.4, we analyze the effect of the hidden dimension size. Experiment details are given in Appendix 9.2.

Datasets. We analyze the quality of representations learned by AF-GCL on transductive node classification benchmarks. Specifically, we evaluate the performance of using the pretraining representations on 8 benchmark homophilic graph datasets, namely, Cora, Citeseer, Pubmed [1] and Wiki-CS, Amazon-Computers, Amazon-Photo, Coauthor-CS, Coauthor-Physics [47], as well as 6 heterophilic graph datasets, namely, Chameleon, Squirrel, Actor [37], Twitch-DE, Twitch-gamers, and Genius [48]. The datasets are collected from real-world networks from different domains; their detailed statistics are summarized in Table 7 and the detailed descriptions are in Appendix 9.1.

Baselines. We consider representative baseline methods belonging to the following three categories (1) Traditional unsupervised graph embedding methods, including DeepWalk [49] and Node2Vec [50], (2) Self-supervised learning algorithms with graph neural networks including Graph Autoencoders (GAE, VGAE) [5], Deep Graph Infomax (DGI) [36], Graphical Mutual Information Maximization (GMI) [11], and Multi-View Graph Representation Learning (MVGRL) [12], graph contrastive representation learning (GRACE) [14] Graph Contrastive learning with Adaptive augmentation (GCA) [13], Bootstrapped Graph Latents (BGRL) [51], (3) Supervised learning and Semi-supervised learning, e.g., Multilayer Perceptron (MLP) and Graph Convolutional Networks (GCN) [1], where they are trained in an end-to-end fashion.

Protocol. We follow the evaluation protocol of previous state-of-the-art graph contrastive learning approaches. Specifically, for every experiment, we employ the linear evaluation scheme as introduced in [36], where each model is firstly trained in an unsupervised manner; then, the pretrained representations are used to train and test via a simple linear classifier. For the datasets that came with standard train/valid/test splits, we evaluate the models on the public splits. For datasets without standard split, e.g., Amazon-Computers, Amazon-Photo, Coauthor-CS, Coauthor-Physics, we randomly split the datasets, where 10%/10%/80% of nodes are selected for the training, validation, and test set, respectively. For most datasets, we report the averaged test accuracy and standard deviation over 10 runs of classification. While, following the previous works [48, 52], we report the test ROC AUC on genius and Twitch-DE datasets.

Implementation. We employ a two-layer GCN [1] as the encoder for all baselines due to its simplicity. Note, although the GCN will encourage the learning of low-frequency information [19], Ma et al. [46] demonstrated that GCN is enough to capture the information within heterophilic graphs following our Assumption 1. Further, the propagation for a single layer GCN is given by,

$$\text{GCN}_i(\mathbf{X}, \mathbf{A}) = \sigma \left(\bar{\mathbf{D}}^{-\frac{1}{2}} \bar{\mathbf{A}} \bar{\mathbf{D}}^{-\frac{1}{2}} \mathbf{X} \mathbf{W}_i \right),$$

where $\bar{\mathbf{A}} = \mathbf{A} + \mathbf{I}$ is the adjacency matrix with self-loops, $\bar{\mathbf{D}}$ is the degree matrix, σ is a non-linear activation function, such as ReLU, and \mathbf{W}_i is the learnable weight matrix for the i 'th layer. The proposed contrastive loss (Equation (8)) is in expectation format. Its empirical version can be written as,

$$\hat{\mathcal{L}} = -\frac{2}{N \cdot K_{pos}} \sum_i \sum_{i^+}^{K_{pos}} [\mathbf{z}_i^\top \mathbf{z}_{i^+}] + \frac{1}{N \cdot K_{neg}} \sum_j \sum_k^{K_{neg}} [(\mathbf{z}_j^\top \mathbf{z}_k)^2], \quad (12)$$

where to approximate the expectation over negative pairs (second term of Equation (8)), we sample K_{neg} nodes for each node. Notably, the empirical contrastive loss is an unbiased estimation of the Equation (8).

7.1 Performance on Homophilic Graph

The homophilic graph benchmarks have been studied by several previous works [36, 11, 12, 14, 51]. We re-use their configuration and compare AF-GCL with those methods. The result is summarized in Table 3. The augmentation-based GCL methods can outperform the corresponding supervised training model. As we analyzed in Section 4, those methods implicitly perturb the high-frequency information across different augmentation views, and the commonly adopted InfoNCE loss [53] enforce the target GNN model to capture the low-frequency information by enforcing the learned representation invariant with different augmentations. And the low-frequency information contributes to the success of the previous GCL methods on the homophilic graphs, which is aligned with previous analysis [54, 19]. Compare with augmentation-based GCL methods, AF-GCL outperforms previous methods on three datasets and achieves second-best performance on the other datasets, which shows the effectiveness of the augmentation-free design on homophilic graphs. In other words, the proposed contrastive learning objective based on the ‘‘embedding concentration property’’ always demonstrates top-2 accuracy among all compared baselines. Note that in our analysis, these baselines are indeed tailored for homophilic graphs and AF-GCL is a theoretically-justified contrastive learning framework without augmentations.

7.2 Performance on Heterophilic Graph

We further assess the model performance on heterophilic graph benchmarks that introduced by Pei et al. [37] and Lim et al. [52]. Different from the experiments on homophilic graphs, existing contrastive

learning methods cannot outperform a vanilla supervised GCN on most of the datasets. As shown in Table 4, AF-GCL achieves the best performance on 5 of 6 heterophilic graphs by an evident margin. For the Twitch-gamers dataset, AF-GCL is competitive with the best one, since it is the heterophilic dataset with the highest node homophily degree. The relatively high homophilic property allows the previous method to work well. Besides, we notice that for the two graphs with the lowest homophily degree, Chameleon and Squirrel, AF-GCL outperform the previous methods with a large margin. The result verifies that our proposed method is suitable for heterophilic graphs. Interestingly, some of the baselines even cannot scale to some graphs and perform poorly on the others. We believe it is due to the high computational cost and loss of the high-frequency information after graph augmentations, which is an innate deficiency of these methods.

Table 5: Computational requirements on a set of standard benchmark graphs. OOM indicates running out of memory on a 32GB GPU.

Dataset	Coauthor-CS	Coauthor-Phy.	Genius	Twitch-gamers
# Nodes	18,333	34,493	421,961	168,114
# Edges	327,576	991,848	984,979	6,797,557
GRACE	13.21 GB	30.11 GB	OOM	OOM
BGRL	3.10 GB	5.42 GB	8.18 GB	26.22 GB
AF-GCL	2.07 GB	3.21 GB	6.24 GB	22.15 GB

7.3 Computational Complexity Analysis

In order to illustrate the advantages of AF-GCL, we provide a brief comparison of the time and space complexities between AF-GCL, the previous strong contrastive method, GCA [13], and the memory-efficient contrastive method, BGRL [51]. GCA is the advanced version of GRACE [13] and performs a quadratic all-pairs contrastive computation at each update step. BGRL, inspired by the bootstrapped design of contrastive learning methods in CV [23], conducts the pairwise comparison between the embeddings learned by an online encoder and a target encoder. Although BGRL does not require negative examples, the two branch design, two different encoders and four embedding table still need to be kept during training, making it hard to scale.

Consider a graph with N nodes and E edges, and a graph neural network (GNN), f , that compute node embeddings in time and space $O(N + E)$. This property is satisfied by most popular GNN architectures, e.g., convolutional [1], attentional [3], or message-passing [55] networks and have been analyzed in the previous works [51]. BGRL performs four GNN computations per update step, in which twice for the target and online encoders, and twice for each augmentation, and a node-level projection; GCA performs two GNN computations (once for each augmentation), plus a node-level projection. Both methods backpropagate the learning signal twice (once for each augmentation), and we assume the backward pass to be approximately as costly as a forward pass. Both of them will compute the augmented graphs by feature masking and edge masking on the fly, the cost for augmentation computation is nearly the same. Thus the total time and space complexity per update step for BGRL is $6C_{encoder}(E + N) + 4C_{proj}N + C_{prod}N + C_{aug}$ and $4C_{encoder}(E + N) + 4C_{proj}N + C_{prod}N^2 + C_{aug}$ for GCA. The C_{prod} depends on the dimension of node embedding and we assume the node embeddings of all the methods with the same size. For our proposed method, only one GNN encoder is employed and we compute the inner product of b nodes to construct positive samples and K_{pos} and K_{neg} inner product for the loss computation. Then for AF-GCL, we have: $2C_{encoder}(E + N) + 2C_{proj}N + C_{prod}(K_{pos} + K_{neg})^2$. We empirically measure the peak of GPU memory usage of AF-GCL, GCA and BGRL. As a fair comparison, we set the embedding size as 128 for all those methods on the four datasets and keep the other hyper-parameters of the three methods the same as the main experiments. The result is summarized in Table 5.

7.4 Representation Size Analysis

As implied by Theorem 2, a larger hidden dimension leads to better performance. We empirically verify that on four datasets. The result is summarized in Table 6 and we can see that the performance increases consistently with larger K .

Table 6: The performance of AF-GCL with different hidden dimension. The average accuracy over 10 runs is reported.

	WikiCS	Amz-Comp.	Actor	Twitch-DE
$K = 256$	78.01	88.51	57.90	73.48
$K = 512$	78.95	89.27	58.83	74.15
$K = 1024$	79.11	89.79	59.04	74.67

8 Conclusion

In this work, we first investigate the effect of graph augmentation techniques—a crucial part of existing graph contrastive learning algorithms. Specifically, they tend to preserve the low-frequency information and perturb the high-frequency information, which mainly contributes to the success of augmentation-based GCL algorithms on the homophilic graph, but limits its application on the heterophilic graphs. Then, motivated by our theoretical analyses of the features aggregated by Graph Neural Networks, we propose an augmentation-free graph contrastive learning method, AF-GCL, wherein the self-supervision signal is constructed based on the aggregated features. We further provide the theoretical guarantee for the performance of AF-GCL as well as the analysis of its efficacy. Empirically, we show that AF-GCL outperforms state-of-the-art GCL algorithms on 4 out of 8 homophilic graph benchmarks and achieves competitive performance on the remaining 4 datasets. Besides, as the first method which can work well on both homophilic and heterophilic graphs, AF-GCL outperforms all those GCL algorithms and supervised methods on 5 out of 6 heterophilic graph benchmarks and achieve competitive performance on the remaining one. Admittedly, we mainly focus on the node classification problem. We would like to leave the exploration of regression problem and graph classification problem in the future.

References

- [1] Thomas N Kipf and Max Welling. Semi-supervised classification with graph convolutional networks. *arXiv preprint arXiv:1609.02907*, 2016.
- [2] Keyulu Xu, Weihua Hu, Jure Leskovec, and Stefanie Jegelka. How powerful are graph neural networks? *arXiv preprint arXiv:1810.00826*, 2018.
- [3] Petar Veličković, Guillem Cucurull, Arantxa Casanova, Adriana Romero, Pietro Lio, and Yoshua Bengio. Graph attention networks. *arXiv preprint arXiv:1710.10903*, 2017.
- [4] William L Hamilton, Rex Ying, and Jure Leskovec. Inductive representation learning on large graphs. *arXiv preprint arXiv:1706.02216*, 2017.
- [5] Thomas N Kipf and Max Welling. Variational graph auto-encoders. *arXiv preprint arXiv:1611.07308*, 2016.
- [6] Ashish Jaiswal, Ashwin Ramesh Babu, Mohammad Zaki Zadeh, Debapriya Banerjee, and Fillia Makedon. A survey on contrastive self-supervised learning. *Technologies*, 9(1):2, 2021.
- [7] Yaochen Xie, Zhao Xu, Jingtun Zhang, Zhengyang Wang, and Shuiwang Ji. Self-supervised learning of graph neural networks: A unified review. *arXiv preprint arXiv:2102.10757*, 2021.
- [8] Ryuichiro Hataya, Jan Zdenek, Kazuki Yoshizoe, and Hideki Nakayama. Faster autoaugment: Learning augmentation strategies using backpropagation. In *European Conference on Computer Vision*, pages 1–16. Springer, 2020.
- [9] Sungbin Lim, Ildoo Kim, Taesup Kim, Chiheon Kim, and Sungwoong Kim. Fast autoaugment. *Advances in Neural Information Processing Systems*, 32:6665–6675, 2019.
- [10] Yuning You, Tianlong Chen, Yongduo Sui, Ting Chen, Zhangyang Wang, and Yang Shen. Graph contrastive learning with augmentations. *Advances in Neural Information Processing Systems*, 33:5812–5823, 2020.
- [11] Zhen Peng, Wenbing Huang, Minnan Luo, Qinghua Zheng, Yu Rong, Tingyang Xu, and Junzhou Huang. Graph representation learning via graphical mutual information maximization. In *Proceedings of The Web Conference 2020*, pages 259–270, 2020.

- [12] Kaveh Hassani and Amir Hosein Khasahmadi. Contrastive multi-view representation learning on graphs. In *International Conference on Machine Learning*, pages 4116–4126. PMLR, 2020.
- [13] Yanqiao Zhu, Yichen Xu, Feng Yu, Qiang Liu, Shu Wu, and Liang Wang. Graph contrastive learning with adaptive augmentation. In *Proceedings of the Web Conference 2021*, pages 2069–2080, 2021.
- [14] Yanqiao Zhu, Yichen Xu, Feng Yu, Qiang Liu, Shu Wu, and Liang Wang. Deep graph contrastive representation learning. *arXiv preprint arXiv:2006.04131*, 2020.
- [15] Qi Zhu, Yidan Xu, Haonan Wang, Chao Zhang, Jiawei Han, and Carl Yang. Transfer learning of graph neural networks with ego-graph information maximization. *arXiv preprint arXiv:2009.05204*, 2020.
- [16] Yanqiao Zhu, Yichen Xu, Qiang Liu, and Shu Wu. An empirical study of graph contrastive learning. 2021.
- [17] Miller McPherson, Lynn Smith-Lovin, and James M Cook. Birds of a feather: Homophily in social networks. *Annual review of sociology*, 27(1):415–444, 2001.
- [18] Jiong Zhu, Yujun Yan, Lingxiao Zhao, Mark Heimann, Leman Akoglu, and Danai Koutra. Beyond homophily in graph neural networks: Current limitations and effective designs. *arXiv preprint arXiv:2006.11468*, 2020.
- [19] Muhammet Balcilar, Guillaume Renton, Pierre Héroux, Benoit Gaüzère, Sébastien Adam, and Paul Honeine. Analyzing the expressive power of graph neural networks in a spectral perspective. In *International Conference on Learning Representations*, 2020.
- [20] Deyu Bo, Xiao Wang, Chuan Shi, and Huawei Shen. Beyond low-frequency information in graph convolutional networks. *arXiv preprint arXiv:2101.00797*, 2021.
- [21] Shouheng Li, Dongwoo Kim, and Qing Wang. Beyond low-pass filters: Adaptive feature propagation on graphs. In *Joint European Conference on Machine Learning and Knowledge Discovery in Databases*, pages 450–465. Springer, 2021.
- [22] Jiezhong Qiu, Qibin Chen, Yuxiao Dong, Jing Zhang, Hongxia Yang, Ming Ding, Kuansan Wang, and Jie Tang. Gcc: Graph contrastive coding for graph neural network pre-training. In *Proceedings of the 26th ACM SIGKDD International Conference on Knowledge Discovery & Data Mining*, pages 1150–1160, 2020.
- [23] Jean-Bastien Grill, Florian Strub, Florent Altché, Corentin Tallec, Pierre Richemond, Elena Buchatskaya, Carl Doersch, Bernardo Avila Pires, Zhaohan Guo, Mohammad Gheshlaghi Azar, et al. Bootstrap your own latent—a new approach to self-supervised learning. *Advances in Neural Information Processing Systems*, 33:21271–21284, 2020.
- [24] Sanjeev Arora, Hrishikesh Khandeparkar, Mikhail Khodak, Orestis Plevrakis, and Nikunj Saunshi. A theoretical analysis of contrastive unsupervised representation learning. *arXiv preprint arXiv:1902.09229*, 2019.
- [25] Jason D Lee, Qi Lei, Nikunj Saunshi, and Jiacheng Zhuo. Predicting what you already know helps: Provable self-supervised learning. *arXiv preprint arXiv:2008.01064*, 2020.
- [26] Christopher Tosh, Akshay Krishnamurthy, and Daniel Hsu. Contrastive learning, multi-view redundancy, and linear models. In *Algorithmic Learning Theory*, pages 1179–1206. PMLR, 2021.
- [27] Yao-Hung Hubert Tsai, Yue Wu, Ruslan Salakhutdinov, and Louis-Philippe Morency. Self-supervised learning from a multi-view perspective. *arXiv preprint arXiv:2006.05576*, 2020.
- [28] Tongzhou Wang and Phillip Isola. Understanding contrastive representation learning through alignment and uniformity on the hypersphere. In *International Conference on Machine Learning*, pages 9929–9939. PMLR, 2020.
- [29] Jeff Z HaoChen, Colin Wei, Adrien Gaidon, and Tengyu Ma. Provable guarantees for self-supervised deep learning with spectral contrastive loss. *arXiv preprint arXiv:2106.04156*, 2021.
- [30] Prannay Khosla, Piotr Teterwak, Chen Wang, Aaron Sarna, Yonglong Tian, Phillip Isola, Aaron Maschinot, Ce Liu, and Dilip Krishnan. Supervised contrastive learning. *arXiv preprint arXiv:2004.11362*, 2020.

- [31] Aaron van den Oord, Yazhe Li, and Oriol Vinyals. Representation learning with contrastive predictive coding. *arXiv preprint arXiv:1807.03748*, 2018.
- [32] Ralph Linsker. Self-organization in a perceptual network. *Computer*, 21(3):105–117, 1988.
- [33] Michael Gutmann and Aapo Hyvärinen. Noise-contrastive estimation: A new estimation principle for unnormalized statistical models. In *Proceedings of the thirteenth international conference on artificial intelligence and statistics*, pages 297–304. JMLR Workshop and Conference Proceedings, 2010.
- [34] Sebastian Nowozin, Botond Cseke, and Ryota Tomioka. f-gan: Training generative neural samplers using variational divergence minimization. In *Proceedings of the 30th International Conference on Neural Information Processing Systems*, pages 271–279, 2016.
- [35] Ben Poole, Sherjil Ozair, Aaron Van Den Oord, Alex Alemi, and George Tucker. On variational bounds of mutual information. In *International Conference on Machine Learning*, pages 5171–5180. PMLR, 2019.
- [36] Petar Velickovic, William Fedus, William L Hamilton, Pietro Liò, Yoshua Bengio, and R Devon Hjelm. Deep graph infomax. *ICLR (Poster)*, 2(3):4, 2019.
- [37] Hongbin Pei, Bingzhe Wei, Kevin Chen-Chuan Chang, Yu Lei, and Bo Yang. Geom-gcn: Geometric graph convolutional networks. *arXiv preprint arXiv:2002.05287*, 2020.
- [38] Negin Entezari, Saba A Al-Sayouri, Amirali Darvishzadeh, and Evangelos E Papalexakis. All you need is low (rank) defending against adversarial attacks on graphs. In *Proceedings of the 13th International Conference on Web Search and Data Mining*, pages 169–177, 2020.
- [39] Prithviraj Sen, Galileo Namata, Mustafa Bilgic, Lise Getoor, Brian Galligher, and Tina Eliassi-Rad. Collective classification in network data. *AI magazine*, 29(3):93–93, 2008.
- [40] Galileo Namata, Ben London, Lise Getoor, Bert Huang, and UMD EDU. Query-driven active surveying for collective classification. In *10th International Workshop on Mining and Learning with Graphs*, volume 8, page 1, 2012.
- [41] Benedek Rozemberczki and Rik Sarkar. Twitch gamers: a dataset for evaluating proximity preserving and structural role-based node embeddings. *arXiv preprint arXiv:2101.03091*, 2021.
- [42] Heng Chang, Yu Rong, Tingyang Xu, Yatao Bian, Shiji Zhou, Xin Wang, Junzhou Huang, and Wenwu Zhu. Not all low-pass filters are robust in graph convolutional networks. *Advances in Neural Information Processing Systems*, 34, 2021.
- [43] Yash Deshpande, Subhabrata Sen, Andrea Montanari, and Elchanan Mossel. Contextual stochastic block models. *Advances in Neural Information Processing Systems*, 31, 2018.
- [44] Aseem Baranwal, Kimon Fountoulakis, and Aukosh Jagannath. Graph convolution for semi-supervised classification: Improved linear separability and out-of-distribution generalization. *arXiv preprint arXiv:2102.06966*, 2021.
- [45] Douglas A Reynolds. Gaussian mixture models. *Encyclopedia of biometrics*, 741(659-663), 2009.
- [46] Yao Ma, Xiaorui Liu, Neil Shah, and Jiliang Tang. Is homophily a necessity for graph neural networks? *arXiv preprint arXiv:2106.06134*, 2021.
- [47] Oleksandr Shchur, Maximilian Mumme, Aleksandar Bojchevski, and Stephan Günnemann. Pitfalls of graph neural network evaluation. *arXiv preprint arXiv:1811.05868*, 2018.
- [48] Derek Lim, Xiuyu Li, Felix Hohne, and Ser-Nam Lim. New benchmarks for learning on non-homophilous graphs. *arXiv preprint arXiv:2104.01404*, 2021.
- [49] Bryan Perozzi, Rami Al-Rfou, and Steven Skiena. Deepwalk: Online learning of social representations. In *Proceedings of the 20th ACM SIGKDD international conference on Knowledge discovery and data mining*, pages 701–710, 2014.
- [50] Aditya Grover and Jure Leskovec. node2vec: Scalable feature learning for networks. In *Proceedings of the 22nd ACM SIGKDD international conference on Knowledge discovery and data mining*, pages 855–864, 2016.
- [51] Shantanu Thakoor, Corentin Tallec, Mohammad Gheshlaghi Azar, Rémi Munos, Petar Veličković, and Michal Valko. Bootstrapped representation learning on graphs. *arXiv preprint arXiv:2102.06514*, 2021.

- [52] Derek Lim, Felix Hohne, Xiuyu Li, Sijia Linda Huang, Vaishnavi Gupta, Omkar Bhalerao, and Ser Nam Lim. Large scale learning on non-homophilous graphs: New benchmarks and strong simple methods. *Advances in Neural Information Processing Systems*, 34, 2021.
- [53] Aaron Van den Oord, Yazhe Li, and Oriol Vinyals. Representation learning with contrastive predictive coding. *arXiv e-prints*, pages arXiv–1807, 2018.
- [54] Hoang Nt and Takanori Maehara. Revisiting graph neural networks: All we have is low-pass filters. *arXiv preprint arXiv:1905.09550*, 2019.
- [55] Justin Gilmer, Samuel S Schoenholz, Patrick F Riley, Oriol Vinyals, and George E Dahl. Neural message passing for quantum chemistry. In *International conference on machine learning*, pages 1263–1272. PMLR, 2017.
- [56] Matthias Fey and Jan Eric Lenssen. Fast graph representation learning with pytorch geometric. *arXiv preprint arXiv:1903.02428*, 2019.
- [57] Adam Paszke, Sam Gross, Soumith Chintala, Gregory Chanan, Edward Yang, Zachary DeVito, Zeming Lin, Alban Desmaison, Luca Antiga, and Adam Lerer. Automatic differentiation in pytorch. 2017.
- [58] Carl Eckart and Gale Young. The approximation of one matrix by another of lower rank. *Psychometrika*, 1(3):211–218, 1936.

9 Appendix

9.1 Dataset Information

We evaluate our models on eight node classification homophilic benchmarks: Cora, Citeseer, Pubmed, WikiCS, Coauthor-CS, Coauthor-Physics, Amazon-Computer and Amazon-Photo and seven non-homophilic benchmarks: Chameleon, Squirrel, Deezer, Penn94 (FB100), Twitch-gamers, Twitch-DE, Genius. The datasets are collected from real-world networks from different domains and we provide dataset statistics in Table 7. For the 8 homophilic graph data, we use the processed version provided by PyTorch Geometric [56]. Besides, for the 6 heterophilic graph data, 3 of them, e.g., Chameleon, Squirrel and Actor are provided by PyTorch Geometric. The other three dataset, genius, twitch-DE and twitch-gamers can be obtained from the official github repository², in which the standard splits for all the 6 heterophilic graph datasets can also be obtained.

Table 7: Statistics of datasets used in experiments.

Name	Nodes	Edges	Classes	Feat.	h_{node}	h_{edge}
Cora	2,708	10,556	7	1,433	.825	.810
CiteSeer	3,327	9,228	6	3,703	.717	.736
PubMed	19,717	88,651	3	500	.792	.802
Coauthor CS	18,333	327,576	15	6,805	.832	.808
Coauthor Phy.	34,493	991,848	5	8,451	.915	.931
Amazon Comp.	13,752	574,418	10	767	.785	.777
Amazon Photo	7,650	287,326	8	745	.836	.827
Chameleon	2,277	36,101	5	2,325	.103	.234
Squirrel	5,201	216,933	5	2,089	.088	.223
Actor	7,600	33,544	5	9,31	.154	.216
Twitch-DE	9,498	153,138	2	2,514	.529	.632
Twitch-gamers	168,114	6,797,557	2	7	.552	.545
Genius	421,961	984,979	2	12	.477	.618

9.2 Implementation Details

Model Architecture and hyperparamters. As we described in Section 7, we employ a two-layer GCN [1] as the encoder for all methods. Following the previous works [1, 48, 52], we apply the l2-normalization for the raw features before training and use batch normalization within the graph encoder. The hyperparameters setting for all experiments are summarized in Table 8. We would like to release our code after acceptance.

Linear evaluation of embeddings. In the linear evaluation protocol, the final evaluation is over representations obtained from pretrained model. When fitting the linear classifier on top of the frozen learned embeddings, the gradient will not flow back to the encoder. We optimize the one layer linear classifier 1000 epochs using Adam with learning rate 0.0005.

Hardware and software infrastructures. Our model are implemented with PyTorch Geometric 2.0.3 [56], PyTorch 1.9.0 [57]. We conduct experiments on a computer server with four NVIDIA Tesla V100 SXM2 GPUs (with 32GB memory each) and twelve Intel Xeon Gold 6240R 2.40GHz CPUs.

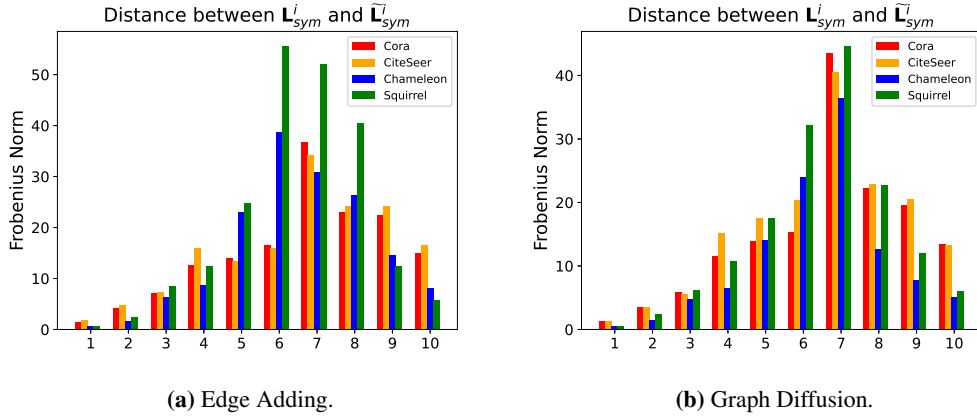
9.3 More Results for the Study of Graph Augmentation

We decomposed the Laplacian matrix into 10 parts and compute the average Frobenius distance for each part over 10 independent runs. As shown in Figure 4a and Figure 4b, both the edge adding with 20% edges and diffusion with $\alpha = 0.2$ have less impact on the low frequency components.

²<https://github.com/CUAI/Non-Homophily-Large-Scale>

Table 8: Hyperparameter settings for all experiments.

	lr.	K_{pos}	K_{neg}	b	T	K
Cora	.0022	5	100	256	2	512
CiteSeer	.0022	10	100	256	2	512
PubMed	.002	10	100	512	2	512
WikiCS	.0016	5	100	512	2	512
Amz-Comp.	.0016	5	100	256	2	512
Amz-Photo	.0021	5	100	512	2	512
Coauthor-CS	.0016	5	100	256	2	512
Coauthor-Phy.	.0021	5	100	512	2	512
Chameleon	.0025	5	100	256	3	512
Squirrel	.0025	5	100	256	3	512
Actor	.0025	10	100	256	4	512
Twitch-DE	.0025	10	100	256	4	512
Twitch-gamers	.0025	5	100	256	4	128
Genius	.0025	10	100	256	3	512



9.4 Detailed Proofs

9.4.1 Proof of Lemma 1

Proof. We first calculate the expectation of aggregated embedding:

$$\mathbb{E}[f_\theta(\mathbf{x}_i)] = \mathbb{E}\left[\mathbf{W} \sum_{j \in \mathcal{N}(i)} \frac{1}{\mathbf{D}_{ii}} \mathbf{x}_j\right] = \mathbf{W} \mathbb{E}_{y \sim P_{y_i}, \mathbf{x} \sim P_y(\mathbf{x})}[\mathbf{x}] \quad (13)$$

This equation is based on the assumption 1 such that $\mathbf{x}_j \sim P_{y_i}(\mathbf{x})$ for every j . Now we provide a concentration analysis. Because each feature \mathbf{x}_i is a sub-Gaussian variable, then by Hoeffding's inequality, with probability at least $1 - \delta'$ for each $d \in [1, F]$, we have,

$$\left| \frac{1}{\mathbf{D}_{ii}} \sum_j (\mathbf{x}_{j,d} - \mathbb{E}[\mathbf{x}_{j,d}]) \right| \leq \sqrt{\frac{\log(2/\delta')}{2\mathbf{D}_{ii} \|\mathbf{x}_{j,d}\|_{\psi_2}}} \quad (14)$$

where $\|\mathbf{x}_{j,d}\|_{\psi_2}$ is sub-Gaussian norm of $\mathbf{x}_{j,d}$. Furthermore, because each dimension of \mathbf{x}_j is i.i.d., thus we define $\|\mathbf{x}_j\|_{\psi_2} = \|\mathbf{x}_{j,d}\|_{\psi_2}$. Then we apply a union bound by setting $\delta' = F\delta$ on the feature dimension k . Then with probability at least $1 - \delta$ we have

$$\left| \frac{1}{\mathbf{D}_{ii}} \sum_j (\mathbf{x}_{j,d} - \mathbb{E}[\mathbf{x}_{j,d}]) \right| \leq \sqrt{\frac{\log(2F/\delta)}{2\mathbf{D}_{ii} \|\mathbf{x}\|_{\psi_2}}} \quad (15)$$

Next, we use the matrix perturbation theory,

$$\begin{aligned} \left\| \frac{1}{\mathbf{D}_{ii}} \sum_j (\mathbf{x}_{j,d} - \mathbb{E}[\mathbf{x}_{j,d}]) \right\|_2 &\leq \sqrt{F} \left\| \frac{1}{\mathbf{D}_{ii}} \sum_j (\mathbf{x}_{j,d} - \mathbb{E}[\mathbf{x}_{j,d}]) \right\| \\ &\leq \sqrt{\frac{F \log(2F/\delta)}{2\mathbf{D}_{ii} \|\mathbf{x}\|_{\psi_2}}} \end{aligned} \quad (16)$$

Finally, plug the weight matrix into the inequality,

$$\|f_\theta(\mathbf{x}_i) - \mathbb{E}[f_\theta(\mathbf{x}_i)]\| \leq \sigma_{\max}(\mathbf{W}) \left\| \frac{1}{\mathbf{D}_{ii}} \sum_j (\mathbf{x}_{j,k} - \mathbb{E}[\mathbf{x}_{j,k}]) \right\|_2 \quad (17)$$

where σ_{\max} is the largest singular value of weight matrix.

9.4.2 Proof of Theorem 1

Proof. The concentration analysis is based on the result obtained in Lemma 1. We first write down the detailed expression for each pair of i, j ,

$$s_{i,j} \equiv \mathbf{x}_i^\top \mathbf{W}^\top \mathbf{W} \mathbf{x}_j \quad (18)$$

We first bound $\mathbf{x}_i^\top \mathbf{x}_j$. Because \mathbf{x}_i and \mathbf{x}_j are independently sampled from an identical distribution, then the product $\mathbf{x}_i^\top \mathbf{x}_j$ is sub-exponential. This can be seen from Orlicz norms relation that $\|x^2\|_{\psi_1} = (\|x\|_{\psi_2})^2$, where $\|\mathbf{x}\|_{\psi_2}$ is sub-exponential norm of \mathbf{x}^2 . Then by the Hoeffding's inequality for sub-exponential variable, with a probability at least $1 - \delta$, we have

$$|\mathbf{x}_i^\top \mathbf{x}_j - \mathbb{E}_{\mathbf{x}_i \sim P_{y_i}, \mathbf{x}_j \sim P_{y_j}}[\mathbf{x}_i^\top \mathbf{x}_j]| \leq \sqrt{\frac{\sigma_{\max}^2(\mathbf{W}^\top \mathbf{W}) \log(2/\delta)}{2\|\mathbf{x}^2\|_{\psi_1}}} \quad (19)$$

Because that the aggregated feature is normalized by the degree of corresponding node, we have, for each pair of i, j

$$|s_{i,j} - \mathbb{E}[s_{i,j}]| \leq \sqrt{\frac{\log(2/\delta) \sigma_{\max}^2(\mathbf{W}^\top \mathbf{W})}{2\|\mathbf{x}^2\|_{\psi_1} \mathbf{D}_{ii} \mathbf{D}_{jj}}} \leq \sqrt{\frac{\sigma_{\max}^2(\mathbf{W}^\top \mathbf{W}) \log(2/\delta)}{2\|\mathbf{x}^2\|_{\psi_1} D^2}} \quad (20)$$

where $D = \min_i \mathbf{D}_{ii}$ for $i \in [1, N]$. Finally we apply a union bound over a pair of i, j . Then with probability at least $1 - \delta$ we have

$$|\mathbf{Z}_i^\top \mathbf{Z}_j - \mathbb{E}[\mathbf{Z}_i^\top \mathbf{Z}_j]| \leq \sqrt{\frac{\sigma_{\max}^2(\mathbf{W}^\top \mathbf{W}) \log(2N^2/\delta)}{2D^2 \|\mathbf{x}^2\|_{\psi_1}}} \quad (21)$$

9.4.3 Proof of Lemma 2

To prove this lemma, we first introduce the concept of the probability adjacency matrix. For the transformed graph $\widehat{\mathcal{G}}$, we denote its probability adjacency matrix as $\widehat{\mathbf{W}}$, in which $\widehat{w}_{ij} = \frac{1}{E} \cdot \widehat{\mathbf{A}}_{ij}$. \widehat{w}_{ij} can be understood as the probability that two nodes have an edge and the weights sum to 1 because the total probability mass is 1: $\sum_{i,j} \widehat{w}_{i,j'} = 1$, for $v_i, v_j \in \mathcal{V}$. Then the corresponding symmetric normalized matrix is $\widehat{\mathbf{W}}_{sym} = \widehat{\mathbf{D}}_{\mathbf{w}}^{-1/2} \widehat{\mathbf{W}} \widehat{\mathbf{D}}_{\mathbf{w}}^{-1/2}$, and the $\widehat{\mathbf{D}} = \text{diag}([\widehat{w}_1, \dots, \widehat{w}_N])$, where $\widehat{w}_i = \sum_j \widehat{w}_{ij}$. We then introduce the Matrix Factorization Loss which is defined as:

$$\min_{\mathbf{F} \in \mathbb{R}^{N \times k}} \mathcal{L}_{mf}(\mathbf{F}) := \left\| \widehat{\mathbf{A}}_{sym} - \mathbf{F} \mathbf{F}^\top \right\|_F^2. \quad (22)$$

By the classical theory on low-rank approximation, Eckart-Young-Mirsky theorem [58], any minimizer $\widehat{\mathbf{F}}$ of $\mathcal{L}_{mf}(\mathbf{F})$ contains scaling of the smallest eigenvectors of \mathbf{L}_{sym} (also, the largest eigenvectors of $\widehat{\mathbf{A}}_{sym}$) up to a right transformation for some orthonormal matrix $\mathbf{R} \in \mathbb{R}^{k \times k}$. We have $\widehat{\mathbf{F}} = \mathbf{F}^* \cdot \text{diag}([\sqrt{1 - \lambda_1}, \dots, \sqrt{1 - \lambda_k}]) \mathbf{R}$, where $\mathbf{F}^* = [\mathbf{u}_1, \mathbf{u}_2, \dots, \mathbf{u}_k] \in \mathbb{R}^{N \times k}$. To proof the Lemma 2, we first present the Lemma 3.

Lemma 3 () *For transformed graph, its probability adjacency matrix, and adjacency matrix are equal after symmetric normalization, $\widehat{\mathbf{W}}_{sym} = \widehat{\mathbf{A}}_{sym}$.*

Proof. For any two nodes $v_i, v_j \in \mathcal{V}$ and $i \neq j$, we denote the the element in i -th row and j -th column of matrix $\widehat{\mathbf{W}}_{sym}$ as $\widehat{\mathbf{W}}_{sym}^{ij}$.

$$\widehat{\mathbf{W}}_{sym}^{ij} = \frac{1}{\sqrt{\sum_k \hat{w}_{ik}} \sqrt{\sum_k \hat{w}_{kj}}} \frac{1}{E} \widehat{\mathbf{A}}^{ij} = \frac{1}{\sqrt{\sum_k \widehat{\mathbf{A}}_{ik}} \sqrt{\sum_k \widehat{\mathbf{A}}_{kj}}} \widehat{\mathbf{A}}^{ij} = \widehat{\mathbf{A}}_{sym}^{ij}. \quad (23)$$

By leveraging the Lemma 3, we present the proof of Lemma 2.

Proof. We start from the matrix factorization loss over $\widehat{\mathbf{A}}_{sym}$ to show the equivalence.

$$\begin{aligned} \|\widehat{\mathbf{A}}_{sym} - \mathbf{F}\mathbf{F}^\top\|_F^2 &= \|\widehat{\mathbf{W}}_{sym} - \mathbf{F}\mathbf{F}^\top\|_F^2 \\ &= \sum_{ij} \left(\frac{\hat{w}_{ij}}{\sqrt{\hat{w}_i} \sqrt{\hat{w}_j}} - f_{mf}(v_i)^\top f_{mf}(v_j) \right)^2 \\ &= \sum_{ij} (f_{mf}(v_i)^\top f_{mf}(v_j))^2 - 2 \sum_{ij} \frac{\hat{w}_{ij}}{\sqrt{\hat{w}_i} \sqrt{\hat{w}_j}} f_{mf}(v_i)^\top f_{mf}(v_j) + \|\widehat{\mathbf{W}}_{sym}\|_F^2 \\ &= \sum_{ij} \hat{w}_i \hat{w}_j \left[\left(\frac{1}{\sqrt{\hat{w}_i}} \cdot f_{mf}(v_i) \right)^\top \left(\frac{1}{\sqrt{\hat{w}_j}} \cdot f_{mf}(v_j) \right) \right]^2 \\ &\quad - 2 \sum_{ij} \hat{w}_{ij} \left(\frac{1}{\sqrt{\hat{w}_i}} \cdot f_{mf}(v_i) \right)^\top \left(\frac{1}{\sqrt{\hat{w}_j}} \cdot f_{mf}(v_j) \right) + C \end{aligned} \quad (24)$$

where $f_{mf}(v_i)$ is the i -th row of the embedding matrix \mathbf{F} . The \hat{w}_i which can be understood as the node selection probability which is proportional to the node degree. Then, we can define the corresponding sampling distribution as P_{deg} . If and only if $\sqrt{\hat{w}_i} \cdot f_\theta \circ g_\omega(v_i) = f_{mf}(v_i) = \mathbf{F}_i$, we have:

$$\begin{aligned} &\mathbb{E}_{\substack{v_i \sim P_{deg} \\ v_j \sim P_{deg}}} \left(f_\theta \circ g_\omega(v_i)^\top f_\theta \circ g_\omega(v_j) \right)^2 \\ &- 2 \mathbb{E}_{\substack{v_i \sim Uni(\mathcal{V}) \\ v_{i+} \sim Uni(\mathcal{N}(v_i))}} \left(f_\theta \circ g_\omega(v_i)^\top f_\theta \circ g_\omega(v_{i+}) \right) + C \end{aligned} \quad (26)$$

where $\mathcal{N}(v_i)$ denotes the neighbor set of node v_i and $Uni(\cdot)$ is the uniform distribution over the given set. Because we constructed the transformed graph by selecting the top- K_{pos} nodes for each node, then all nodes have the same degree. We can further simplify the objective as:

$$\mathbb{E}_{\substack{v_i \sim Uni(\mathcal{V}) \\ v_j \sim Uni(\mathcal{V})}} \left(\mathbf{Z}_i^\top \mathbf{Z}_j \right)^2 - 2 \mathbb{E}_{\substack{v_i \sim Uni(\mathcal{V}) \\ v_{i+} \sim Uni(S_{pos}^i)}} \left(\mathbf{Z}_i^\top \mathbf{Z}_{i+} \right) + C. \quad (27)$$

Due to the node selection procedure, the factor $\sqrt{\hat{w}_i}$ is a constant and can be absorbed by the neural network, $f_\theta \circ g_\omega$. Besides, because $\mathbf{Z}_i = f_\theta \circ g_\omega(v_i)$, we can have the Equation 27. Therefore, the minimizer of matrix factorization loss is equivalent with the minimizer of the contrastive loss.

9.4.4 Proof of Theorem 2

Recently, Haochen et al. [29] presented the following theoretical guarantee for the model learned with the matrix factorization loss.

Lemma 4 () *For a graph \mathcal{G} , let $f_{mf}^* \in \arg \min_{f_{mf}: \mathcal{V} \rightarrow \mathbb{R}^K}$ be a minimizer of the matrix factorization loss, $\mathcal{L}_{mf}(\mathbf{F})$, where $\mathbf{F}_i = f_{mf}(v_i)$. Then, for any label \mathbf{y} , there exists a linear classifier $\mathbf{B}^* \in \mathbb{R}^{c \times K}$ with norm $\|\mathbf{B}^*\|_F \leq 1/(1 - \lambda_K)$ such that*

$$\mathbb{E}_{v_i} \left[\|\vec{y}_i - \mathbf{B}^* f_{mf}^*(v_i)\|_2^2 \right] \leq \frac{\phi^{\mathbf{y}}}{\lambda_{K+1}}, \quad (28)$$

where \vec{y}_i is the one-hot embedding of the label of node v_i . The difference between labels of connected data points is measured by $\phi^{\mathbf{y}}$, $\phi^{\mathbf{y}} := \frac{1}{E} \sum_{v_i, v_j \in \mathcal{V}} \mathbf{A}_{ij} \cdot \mathbb{1}[y_i \neq y_j]$.

Proof. This proof is a direct summary on the established lemmas in previous section. By Lemma 2 and Lemma 4, we have,

$$\mathbb{E}_{v_i} \left[\|\vec{y}_i - \mathbf{B}^* f_{gcl}^*(v_i)\|_2^2 \right] \leq \frac{\phi^{\mathbf{y}}}{\hat{\lambda}_{K+1}} \quad (29)$$

where $\hat{\lambda}_i$ is the i -th smallest eigenvalue of the Laplacian matrix $\hat{\mathbf{L}}_{sym} = \mathbf{I} - \hat{\mathbf{A}}_{sym}$. Note that ϕ^y in Lemma 4 equals $1 - h_{edge}$. Then we apply Theorem 1 and conclude the proof:

$$\mathbb{E}_{v_i} \left[\left\| \vec{y}_i - \mathbf{B}^* f_{\text{gcl}}^*(v) \right\|_2^2 \right] \leq \frac{1 - h_{edge}}{\hat{\lambda}_{K+1}} \leq \frac{\bar{\phi} + \sqrt{\frac{\sigma_{\max}^2(\mathbf{W}^\top \mathbf{W}) \log(2N^2/\delta)}{2D^2 \|\mathbf{x}^2\|_{\psi_1}}}}{\hat{\lambda}_{K+1}} \quad (30)$$